PHYSICAL REVIEW B, VOLUME 64, 081305(R)

Effects of interfacial atomic segregation on optical properties of InAs/GaSb superlattices

Rita Magri
Istituto Nazionale per la Fisica della Materia e Dipartimento di Fisica, Universitá di Modena e Reggio Emilia, Modena, Italy

Alex Zunger
National Renewable Energy Laboratory, Golden, Colorado 80401
(Received 13 March 2001; published 7 August 2001)

Largely because of the lack of detailed microscopic information on the interfacial morphology, most electronic structure calculations on superlattices and quantum wells assume abrupt interfaces. Cross-sectional scanning tunneling microscopy (STM) measurements have now resolved atomic features of segregated interfaces. We fit a layer-by-layer growth model to the observed STM profiles, extracting surface-to-subsurface atomic exchange energies. These are then used to obtain a detailed simulated model of segregated InAs/GaSb superlattices with atomic resolution. Applying pseudopotential calculations to such structures reveals remarkable electronic consequences of segregation, including a blueshift of interband transitions, lowering of polarization anisotropy, and reduction of the amplitude of heavy-hole wave functions at the inverted interface.

DOI: 10.1103/PhysRevB.64.081305 PACS number(s): 71.55.Eq, 73.21.−b

The natural difference in surface energies of the alloy components invariably causes certain atomic species to segregate to the surface during alloy growth. This effect necessarily leads to a structural and chemical asymmetry in quantum wells or superlattices. For example, since In segregates to the surface in preference to Ga, the growth of InAs-on-GaAs can lead to an abrupt interface, whereas the next step of growth of GaAs-on-InAs leads, by necessity, to an intermixed interface as In attempts to float from subsurface layers into the GaAs top layer. This segregation-induced structural asymmetry, noted previously in cation-segregating systems such as AlAs/GaAs and InAs/GaAs,[1,2] leads to significant changes in the optical properties.[3,4] Only recently were such effects explored in anion-segregating systems.[5,6] Of particular interest here is the infrared laser[7] and the light-emitting diode[8] material InAs/GaSb. Since the binary components InAs and GaSb do not share a common element, the two interfaces of an ideal InAs/GaSb quantum well have chemically distinct bonds that do not appear in the respective endpoint components (see inset to Fig. 1). Thus, growth of InAs-on-GaSb (''normal interface'') leads to an interfacial Ga-As bond, whereas growth of GaSb-on-InAs (''inverted interface'') leads to an interfacial In-Sb bond. The ensuing lower (C_{2v}) symmetry relative to common-atom quantum wells (D_{2d}) makes the optical properties of systems without a common atom particularly susceptible to segregation effects. Largely because of lack of atomistic information on the structure of segregated interfaces, electronic structure calculations with only few exceptions,[3,4] have thus far assumed ideal, abrupt, interfaces. To address this issue one needs to (a) quantify the degree of segregation at the interfaces, and (b) establish how does atomic segregation affect the optical properties of the superlattices.

Cross-sectional scanning tunneling microscopy (STM) has made a substantial progress in achieving the first task, identifying the interfacial bonding at GaSb/InAs heterojunctions, and measuring the compositional grading in $Ga_xIn_{1-x}Sb$/InAs superlattices caused by Sb segregation at an atomic level.[6] In this paper we tackle task (b). We first formulate a layer-by-layer growth model, adjusting the atomic segregation energies of In/Ga and Sb/As so as to fit the detailed segregation profile measured[6] by cross-sectional STM for $Ga_xIn_{1-x}Sb$/InAs. We next apply this model to superlattices $(GaSb)_n/(InAs)_m$ (for which optical properties were measured[9]), generating detailed atomistic structures of both ideally abrupt, as well as segregated interfaces, corresponding to a range of growth temperatures. Finally, we apply to these atomistic models of segregated superlattices the pseudopotential electronic structure method, finding the energy levels, wave functions, transition probabilities, and polarization anisotropy. This establishes directly the effect of interfacial segregation on electronic properties. We find the following.

(i) Sb segregates primarily at the ''normal interface,'' whereas In segregates primarily at the ''inverted interface.'' However, some secondary segregation occurs too: As segregates somewhat at the inverted interface, but Ga does not segregate at the normal interface.

(ii) Segregation reduces significantly the amplitude of the wave function of the first heavy hole (hh1) at the inverted interface, hence diminishing significantly the dissimilarity with the normal interface, where hh1 always has a small amplitude. This effect reduces the polarization anisotropy of absorption which reflects this dissimilarity.

(iii) Driven by In segregation, the potential at the inverted interface shifts into the InAs well region, reducing effectively the well width by ≈ 1 ML. This leads to a blueshift of the confined electron states. The potential at the normal interface shows instead a ≈ 2 ML region of disorder. This widens effectively the GaSb hole well width. The former effect is larger than the latter, so the net effect of segregation is a blueshift of the band gap.

To generate composition profiles for GaSb/InAs superlattices we have relied on a kinetic model for molecular-beam epitaxy growth, first introduced, to the best of our knowledge, by Dehaese *et al.*,[10] which we have extended to treat simultaneously segregation both of group III and of group V species in the no-common-atom quaternary GaSb/InAs sys-

 ©2001 The American Physical Society

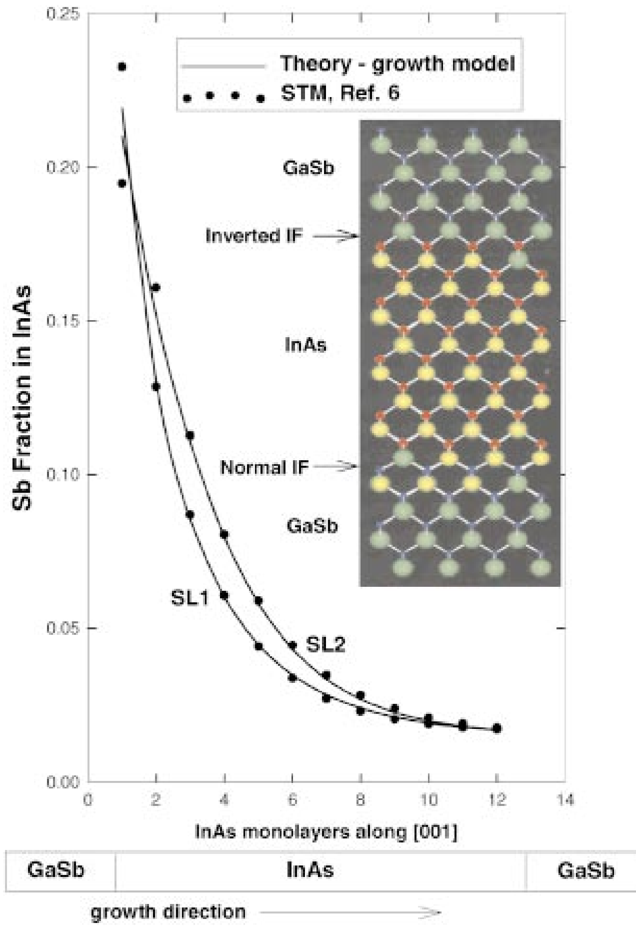

FIG. 1. (Color) Sb composition profiles within the InAs layer of the SL1 and SL2 samples. Lines, results of the growth model; dots, STM data of Ref. 6. The profile SL1 has been obtained using a growth temperature $T_{g1}=380\,^{\circ}\mathrm{C}$, SL2 using $T_{g2}=445\,^{\circ}\mathrm{C}$. In the inset we show a section on a (110) plane of a segregated $(\mathrm{InAs})_8/(\mathrm{GaSb})_8$ superlattice grown at $T_g=400\,^{\circ}\mathrm{C}$. Yellow atoms, As; green atoms, Sb.

tem. The model simulates a layer-by-layer growth starting from a given substrate, and, at each interface, segregation is determined by atomic exchanges between the surface layer and the first subsurface layer, for each sublattice (cation and anion) separately. Layer growth is driven by the impinging atomic fluxes with deposition rates Φ_{In}, Φ_{Ga}, Φ_{Sb}, and Φ_{As} (in ML/s). Atomic exchanges require overcoming energetic barriers for bulk-to-surface ($b\rightarrow s$) and surface-to-bulk ($s\rightarrow b$) atomic swaps. For the cation system we have the barrier $E^{b\rightarrow s}_{In/Ga}$ for subsurface In to exchange with surface Ga, and $E^{s\rightarrow b}_{In/Ga}$ for surface In to exchange with subsurface Ga. Similarly, we have $E^{b\rightarrow s}_{Sb/As}$ and $E^{s\rightarrow b}_{Sb/As}$ with similar meanings. The segregation driving forces are proportional to

$$\Delta_{In/Ga}=E^{s\rightarrow b}_{In/Ga}-E^{b\rightarrow s}_{In/Ga},$$

$$\Delta_{Sb/As}=E^{s\rightarrow b}_{Sb/As}-E^{b\rightarrow s}_{Sb/As}. \tag{1}$$

Here $\Delta_{In/Ga}>0$ (<0) implies In (Ga) segregation to the surface, whereas $\Delta_{Sb/As}>0$ (<0) implies Sb (As) segregation. The rates of $i=b\rightarrow s$ or $i=s\rightarrow b$ exchange reactions at growth temperature T_g are $P_i=\nu_i\exp[-(E^i_{\alpha/\beta})/k_BT_g)]$, where k_B is the Boltzmann constant and ν_i is the effective hopping frequency for which we use the commonly accepted value of $10^{13}\ \mathrm{s}^{-1}$ for III-V compounds.[4,10] Denoting by A and B the two different kinds of atoms in one sublattice (e.g., In and Ga), the rate of change of the concentration $x_A(t)$ of surface A atoms is given by[10]

$$\frac{dx^s_A(t)}{dt}=\Phi_A+P_1x^b_A(t)x^s_B(t)-P_2x^s_A(t)x^b_B(t). \tag{2}$$

Here $x^{s,b}_A(t)$ and $x^{s,b}_B(t)$ are the time-dependent concentrations of A and B at the surface or bulk, the first term Φ_A is the deposition rate of A atoms onto the surface, the second term is the rate of A atoms arriving from subsurface to the surface after exchanging with surface B atoms, and the last term is the rate of A atoms leaving the surface after exchanging with bulk B atoms. The conservation of A atoms and of the total number of surface atoms at any time t leads to the conditions:

$$x^s_A(t)+x^b_A(t)=x^s_A(0)+x^b_A(0)+\Phi_At, \tag{3}$$

$$x^s_A(t)+x^s_B(t)=x^s_A(0)+x^s_B(0)+(\Phi_A+\Phi_B)t, \tag{4}$$

and, at any t, we have $x^b_A(t)+x^b_B(t)=1$. A small fraction x_0 of the segregating Sb species is incorporated into each InAs layer during the growth because of an unwanted vapor background. This cross incorporation has been taken into account modifying slightly the fluxes Φ_{As} and Φ_{Sb} during the growth of InAs so as to have the incorporation of a small constant Sb fraction $x_0=0.015$ into each InAs layer, as proposed in Ref. 6. Our approximations are (i) the barrier energies, Eq. (1), for atomic exchanges are assumed to be independent on the atomic species surrounding the exchanging atoms, and (ii) surface reconstructions during growth are neglected, so the results for the first monolayer, (where reconstruction occurs) might be less reliable than others.

We solve numerically Eqs. (2)–(4) for $A=$ Ga, In, As, and Sb. The input to the simulation consists of growth temperature T_g, atomic fluxes Φ_α, $\alpha=$ Ga, In, As, and Sb, and the four exchange energies appearing in Eq. (1). A single deposition rate of 0.25 ML/s has been used. The two exchange energies for cation $E^i_{In/Ga}$ are taken as the values proposed in previous papers:[10] $E^{b\rightarrow s}_{In/Ga}=1.8$ eV and $E^{s\rightarrow b}_{In/Ga}=2.0$ eV; $\Delta_{In/Ga}>0$ implies In segregation. No values for $E^{b\rightarrow s}_{Sb/As}$ and $E^{s\rightarrow b}_{Sb/As}$ have been previously reported in the literature, so we fix them by fitting the growth model to the experimental Sb concentration profiles measured via cross-sectional STM (Fig. 4 of Ref. 6). The profiles were measured for two different samples: SL1, $(\mathrm{GaIn}_{0.25}\mathrm{Sb})_{6.5}/(\mathrm{InAs})_{15.5}$, at a growth temperature 380 °C, and SL2, $(\mathrm{GaIn}_{0.23}\mathrm{Sb})_6/(\mathrm{InAs})_{14}$, at a growth temperature 440 °C. The dots in Fig. 1 show the two measured segregation profiles. The fit (lines in Fig. 1) to the experimental profiles gives $E^{b\rightarrow s}_{Sb/As}=1.68$ eV and $E^{s\rightarrow b}_{Sb/As}=1.75$ eV. The fit is excellent except for the very first monolayer, where we neglected reconstruction. Our determined $\Delta_{Sb/As}>0$ shows that Sb segregates into the InAs layer, as observed.[6] $E^{b\rightarrow s}_{Sb/As}$ and $E^{s\rightarrow b}_{Sb/As}$ are both smaller than $E^{b\rightarrow s}_{In/Ga}$

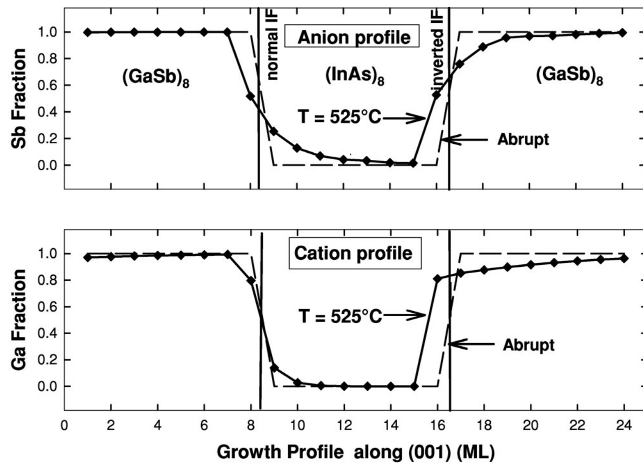

FIG. 2. Sb and Ga composition profiles along the superlattice growth direction for a $(InAs)_8/(GaSb)_{16}$ superlattice grown at $T_g = 525\,°C$. The segregated profile (diamond plus continuous line) is compared with the profile of a superlattice with abrupt interfaces (dashed lines).

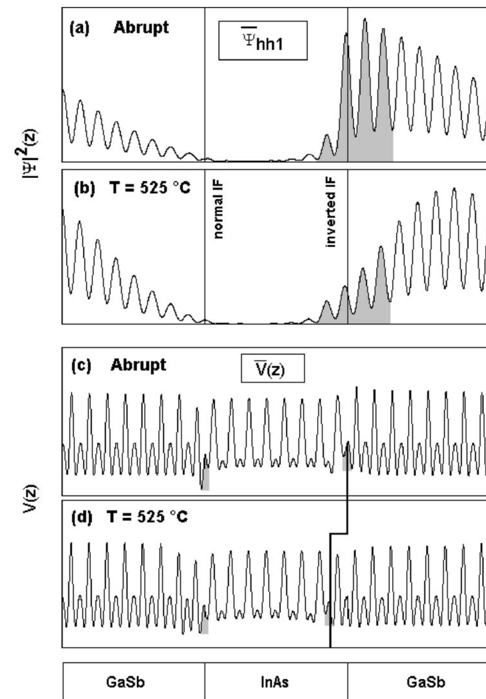

FIG. 3. Comparison of the in-plane-averaged amplitude of the hh1 wave function along the growth direction in (a) a $(InAs)_8/(GaSb)_{16}$ superlattice with abrupt interfaces and (b) a segregated $(InAs)_8/(GaSb)_{16}$ superlattice grown at $T_g = 525\,°C$. Shaded areas stress the differences of amplitude on the inverted interface. Comparison of the in-plane averaged potential for the same superlattices: (c) abrupt geometry and (d) segregated geometry.

and $E^{s\rightarrow b}_{In/Ga}$, so at very low growth temperatures ($<375\,°C$) only anion segregation will be important, whereas appreciable In segregation is expected at higher temperatures ($>375\,°C$).

Having obtained the segregation parameters for the InAs/GaSb system, we next model the atomistic structure of the superlattices used for optical studies.[10] We consider (001) $(InAs)_8/(GaSb)_{16}$ and $(InAs)_8/(GaSb)_8$ superlattices lattice matched to a GaSb substrate. While we have modeled the profile along the [001] growth direction (e.g., Fig. 1) no experimental information is available on the atomistic arrangement in the perpendicular substrate (001) plane. We thus assume random arrangements in these planes, consistent with the planar composition profile dictated by the growth model. To achieve this we use a surface unit cell containing 16 atoms in the (001) plane, which are distributed randomly. Once we determine the superlattice configuration consistent with the solution of the growth model at a given growth temperature T_g, we permit local atomic displacements by a valence force field approach.[11]

Figure 2 shows the anion and cation segregation profiles obtained for a $(InAs)_8/(GaSb)_{16}$ superlattice at an high growth temperature. We see the following.

(i) Segregation leads to the penetration of Sb and In deeply into the InAs and GaSb layers, respectively. The penetration length increases with growth temperatures. At $T_g = 525\,°C$, Sb penetrates 5–6 ML into InAs, while In penetration length is much larger (because of the larger $\Delta_{In/Ga}$), being about 11 ML.

(ii) Sb segregation occurs primarily at the normal interfaces (InAs-on-GaSb) where in the abrupt geometry a Ga-As bond exists, while In segregation occurs at the inverted interface (GaSb-on-InAs), where in the abrupt geometry an In-Sb bond exixts. Our profiles at low ($400\,°C$) growth temperatures closely agree with the STM images of the anion sublattice of Ref. 6 where it is seen that the anion intermixing is much larger at the normal interfaces than at the inverted interfaces[6] (see inset in Fig. 1).

(iii) There is also a substantial anion intermixing at the inverted interface and a (smaller) cation intermixing at the normal interface. This is related to the difference $\Delta_{In/Ga}$ and $\Delta_{Sb/As}$ between the barrier energies [Eq. (1). If Δ is small, the segregation of the species with a higher energy barrier (i.e., As) becomes noticeable at high T_g. We find $\Delta_{Sb/As} = 70$ meV, while $\Delta_{In/Ga}$ is much larger, 200 meV. This explains why at high T_g the anion profile at the inverted interface is more broadened (for As segregation) than the analogous cation profile at the normal interface (no Ga segregation). We will see below, that segregation at the *inverted interface* leads to a narrowing of the InAs well.

Using the calculated segregation profiles we generate detailed atomistic models for different growth temperatures. The electronic and optical properties of such structures are then obtained using the pseudopotential method.[12] The atomic pseudopotentials are obtained fitting the observed band gaps, effective masses, and deformation potentials of the constituent bulk binaries: GaSb, InAs, InSb, and GaAs.[13] Spin-orbit coupling is included as in Ref. 14.

Figures 3(a) and 3(b) shows the square of the (xy-averaged) wave functions of the hh1 hole state of the $(InAs)_8/(GaSb)_{16}$ superlattice. We see that the hh1 wave function is strongly affected by segregation: whereas in the

abrupt geometry (3a), the hh1 amplitude on the normal interface is much smaller than that on the inverted interface, in the segregated geometry (3b) the amplitude of hh1 on the inverted interface is reduced substantially and becomes similar to the amplitude on the normal interface. Segregation affects to a lesser degree the lh1 and *e*1 wave functions (not shown). Another interesting result is related to the behavior of the potential [Figs. 3(b) and 3(d)]: segregation affects mostly the inverted interface where there is a shift of the interface itself and the InAs well becomes 1 ML narrower.

The interband transition energies and dipole oscillator strengths at the Brillouin-zone center have been calculated as a function of the growth temperature for the $(InAs)_8/(GaSb)_{16}$ superlattice (Fig. 4). We see the following.

(1) A segregation-induced *increase* (blueshift) of the interband transition energies with growth temperature until $T_g = 425\,°C$. The blueshift is due to the narrowing of the InAs well (for electrons) and the broadening of the GaSb well (for holes) with In segregation. The electron state becomes more confined with increasing T_g, whereas hole states become less confined, but their energies change at a smaller rate, so interband energies increase with T_g. This result explains the surprising gap increase with T_g previously observed for similar structures.[15]

(2) A reduced blueshift at $T_g > 425\,°C$ due to a diminishing of Sb and (at a lesser rate) In segregation because of the competing segregation of As and Ga. This leads to a slight decrease of the interband transition energies.

(3) While the intensity of the hh1 $\rightarrow e1$ interband transition is not affected by segregation, the lh1 $\rightarrow e1$ transition becomes more intense with segregation and correspondingly the (parity forbidden) hh2 $\rightarrow e1$ transition becomes less intense [Fig. 4(b)]. This is because segregation diminishes the lh1-hh2 coupling which makes the nominally forbidden hh2 $\rightarrow e1$ transition of D_{2d} and C_{2v} symmetries slightly allowed.[16]

(4) The calculated polarization ratio $PA = |P_{110} - P_{-110}|/|P_{110} + P_{-110}|$ between the dipole transition element P in the two in-plane orientations [110] and [−110] is reduced with segregation [Fig. 4(c)]. Already at $T_g = 350\,°C$ the PA is much smaller than that relative to the abrupt geometry. The PA decreases until about $T_g = 500\,°C$ in correspondence with the increase of In segregation.

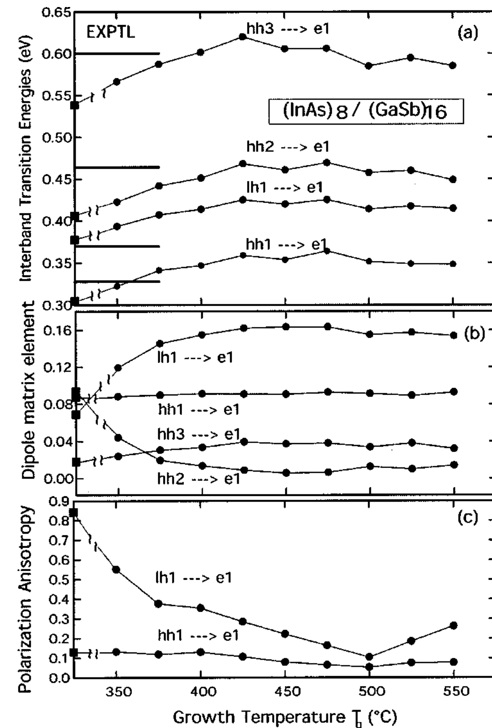

FIG. 4. (a) Energies of the first four interband transitions at the BZ center of the segregated $(InAs)_8/(GaSb)_{16}$ superlattices versus growth temperature. The absorbance spectroscopy data of Ref. 9 are given with horizontal bars on the left side; (b) Dipole oscillator strengths versus growth temperature; (c) In-plane polarization ratio PA of the hh1 $\rightarrow e1$ and lh1 $\rightarrow e1$ transitions versus growth temperature. The corresponding values of the abrupt geometry are given by squares at the far left side of the figure.

The technique of performing electronic structure calculations on simulated atomistic models of nonideal interfaces fit to *X*-STM profiles opens the way for establishing the link between morphology and optical properties of nanostructures.

The work of R.M. was supported by the Italian MURST Project No. COFIN99 and by European INTAS-99-15, whereas the work of A.Z. was supported by DOE-OS-DMS, condensed matter physics.

[1] J. M. Moison *et al.*, Phys. Rev. B **40**, 6149 (1989).
[2] W. Braun *et al.*, Phys. Rev. B **55**, 1689 (1997).
[3] D. B. Laks and A. Zunger, Phys. Rev. B **45**, 14 177 (1992).
[4] B. Koiller *et al.*, Phys. Rev. B **60**, 1787 (1999).
[5] R. Kaspi, J. Cryst. Growth **201/202**, 864 (1999).
[6] J. Steinshnider *et al.*, Phys. Rev. Lett. **85**, 2953 (2000); J. Steinshnider *et al.*, *ibid.* **85**, 4562 (2000).
[7] C.-H Lin *et al.*, Proc. SPIE Int. Soc. Opt. Eng. **3628**, 22 (1998).
[8] R. H. Miles *et al.*, Appl. Phys. Lett. **66**, 1921 (1995).
[9] R. Kaspi *et al.*, Appl. Phys. Lett. **76**, 409 (2000).
[10] O. Dehaese *et al.*, Appl. Phys. Lett. **66**, 52 (1995).
[11] P. N. Keating, Phys. Rev. **145**, 637 (1966).
[12] L. W. Wang *et al.*, Phys. Rev. B **60**, 5590 (1999).
[13] The atomic empirical pseudopotentials of Ref. 12 have been improved, R. Magri and A. Zunger (unpublished).
[14] L. W. Wang and A. Zunger, Phys. Rev. B **51**, 17 398 (1995).
[15] M. J. Yang *et al.*, Electron. Lett. (U.K.) **34**, 270 (1998).
[16] R. Magri and A. Zunger, Phys. Rev. B **62**, 10 364 (2000).